$R_{\rm be}, \beta(\alpha, G_m)$, once the collector and the base–currents are known, remain really close to the fitted ones.

ACKNOWLEDGMENT

The authors acknowledge Siemens for processing the MOVPE-wafers for this work.

REFERENCES

[1] G. Dambrine, A. Cappy, F. Heliodore, and E. Playez, "A new method for determining the FET small-signal equivalent circuit," *IEEE Trans. Microwave Theory Tech.*, vol. 36, July 1988.

[2] D. Costa, W. U. Liu, and J. S. Harris, "Direct extraction of the AlGaAs/GaAs heterojunction bipolar transistor small-signal equivalent circuit," *IEEE Trans. Electron Devices*, vol. 38, Sept. 1991.

[3] R. A. Pucel and U. L. Rohde, "An exact expression for the noise resistance R_n for the Hawkins bipolar noise model," *IEEE Microwave Guided Wave Lett.*, vol. 3, Feb. 1993.

[4] S. Maas, B. L. Nelson, and D. L. Tait, "Intermodulation in heterojunction bipolar transistors," *IEEE Trans. Microwave Theory Tech.*, vol. 40, Mar. 1992.

[5] U. Schaper, K. H. Bachem, M. Karner, and P. Zwicknagl, "Scaling of small-signal equivalent circuit elements for GaInP/GaAs hole-barrier-bipolar-transistors," *IEEE Trans. Electron Devices*, vol. 40, Jan. 1993.

[6] S. A. Maas and D. Tait, "Parameter-extraction method for heterojunction bipolar transistors," *IEEE Microwave Guided Wave Lett.*, vol. 2, Dec. 1992.

[7] S. Lee and A. Gopinath, "Parameter extraction technique for HBT equivalent circuit cutoff mode measurement," *IEEE Trans. Microwave Theory Tech.*, vol. 40, Mar. 1992.

[8] D. R. Pehlke and D. Pavlidis, "Evaluation of the factors determining HBT high-frequency performance by direct analysis of S-parameter data," *IEEE Trans. Microwave Theory Tech.*, vol. 40, Dec. 1992.

A Rigorous Analysis of a Cross Waveguide to Large Circular Waveguide Junction and Its Application in Waveguide Filter Design

Ke-Li Wu and Robert H. MacPhie

***Abstract*—A rigorous analysis is obtained for the problem of scattering at the junction of a cross-shaped waveguide and a larger circular waveguide. The general case of an arbitrary offset and orientation of the cross waveguide axes is considered. The fields matching over the cross aperture of the smaller guide is facilitated by using the transformation of the circular cylindrical Bessel–Fourier modal fields of the circular guide into a finite series of exponential plane wave functions. This permits an analytical finite series solution for the elements of the fields mode matching matrix, from which the general scattering matrix of the junction is obtained. The application of the formulation to circular waveguide filter design is emphasized in the numerical examples. Excellent agreements between theoretical and experimental results are obtained in all the numerical examples.**

***Index Terms*—Modal analysis, waveguide filter design, waveguide junction.**

Manuscript received November 10, 1995. This work was supported in part by the Natural Sciences and Engineering Research Council of Canada.

K.-L. Wu is with Corporate Research and Development Department, COM DEV Ltd., Cambridge, ON N1R 7H5, Canada.

R. H. MacPhie is with Department of Electrical and Computer Engineering, University of Waterloo, Waterloo, ON N2L 3G1, Canada.

Publisher Item Identifier S 0018-9480(97)00431-6.

I. INTRODUCTION

Due to the significant position of narrow bandwidth multimode channel filters in communication satellite payloads [1], rigorous electromagnetic (EM) modeling of the filters has become an urgent task since the circuit theory model [2] was developed by Atia and Williams in the 1970's. An accurate modeling and design of the channel filters will considerably reduce or even hopefully eliminate the manual tuning process. One of the key elements in the EM filter design is the modeling of cross- or rectangular-shaped irises between circular waveguide cavities.

Because of the difficulties engendered by the different geometrical coordinates in the iris aperture and circular waveguides (one is rectangular, another is circular), analysis of these types of junctions has shown that "there appears to be no easy analytical solution" [3] and numerical integration has been used [3]–[5].

Fortunately, an easy analytical solution has been available using a plane-wave finite series expansion of the Bessel–Fourier modal eigenfunction in the circular waveguide [6]. An analytical solution for the scattering of smaller rectangular-to-circular waveguides has been given in [6]. This paper will provide a rigorous analysis of an arbitrary offset and orientation cross waveguide to a large circular waveguide junction. Applications of the analysis to waveguide filter design will be emphasized. This is an extension of the work in [6] to a more practical case in waveguide dual mode filter design.

Instead of treating the horizontal and vertical slots separately, as in [4], the cross-shaped slot will be treated as a complete waveguide. The advantages of the new formulation over previous works are: 1) it provides the coupling information for a slot in one direction in the presence of another slot in the perpendicular direction; 2) the coupling information for both slots can be obtained at same time, which is very important in full EM analysis of circular waveguide dual mode filters; and 3) full analytical expressions to be deduced for the elements of the modal analysis matrix equation lead to a rigorous and efficient solution of the problem.

The formulation has been verified by experiments and excellent agreements are obtained.

II. THEORY

A. Mode Functions in Cross Waveguide

The generalized crossed rectangular waveguide considered in this paper is depicted in Fig. 1(a). The modes in the cross waveguide are grouped according to their symmetry with respect to the x and y axis. The modal solutions have been discussed in [7]. For clarity, the nth mode functions for each group will be summarized in the following compact form:

$$\vec{e}_{ht1}{}^{n} = -N_h^n \sum_r \Phi_{1r}^n \{ \left(\frac{r\pi}{2d}\right) Q[p_{1r}^n(\frac{x}{2a} - \frac{1}{2})] P[\frac{r\pi(d-y)}{2d}]\widehat{x} - \left(\frac{p_{1r}^n}{2a}\right) R[p_{1r}^n(\frac{x}{2a} - \frac{1}{2})] \cdot S[\frac{r\pi(d-y)}{2d}]\widehat{y}\} \tag{1a}$$

$$\vec{e}_{et1}{}^{n} = N_e^n \sum_r \Phi_{1r}^n \{ \left(\frac{p_{1r}^n}{2a}\right) Q[p_{1r}^n(\frac{x}{2a} - \frac{1}{2})] P[\frac{r\pi(d-y)}{2d}]\widehat{x} - \left(\frac{r\pi}{2d}\right) R[p_{1r}^n(\frac{x}{2a} - \frac{1}{2})] \cdot S[\frac{r\pi(d-y)}{2d}]\widehat{y}\} \tag{1b}$$

TABLE I
FUNCTIONS AND BOUNDARY CONDITIONS USED IN (1)

Mode Group	$\substack{TE\\TM}$ *odd, even*	$\substack{TE\\TM}$ *odd, odd*	$\substack{TE\\TM}$ *even, even*	$\substack{TE\\TM}$ *even, odd*
X Axis condition	Electric Wall	Magnetic Wall	Electric Wall	Magnetic Wall
Y Axis condition	Magnetic Wall	Magnetic Wall	Electric Wall	Electric Wall
Mode Index *iqq*	1	2	3	4
Q	$cosh[\cdot]$	$cosh[\cdot]$	$cosh[\cdot]$	$cosh[\cdot]$
P or B	$sin[\cdot]$	$sin[\cdot]$	$sin[\cdot]$	$sin[\cdot]$
R	$sinh[\cdot]$	$sinh[\cdot]$	$sinh[\cdot]$	$sinh[\cdot]$
S or D	$cos[\cdot]$	$cos[\cdot]$	$cos[\cdot]$	$cos[\cdot]$
A	$sinh[\cdot]$	$sinh[\cdot]$	$cosh[\cdot]$	$cosh[\cdot]$
C	$cosh[\cdot]$	$cosh[\cdot]$	$sinh[\cdot]$	$sinh[\cdot]$
Index r or m $\substack{TE\\TM}$	0,2,4,6,... 2,4,6,...	1,3,5,... 1,3,5,...	0,2,4,6,... 2,4,6,...	1,3,5,... 1,3,5,...

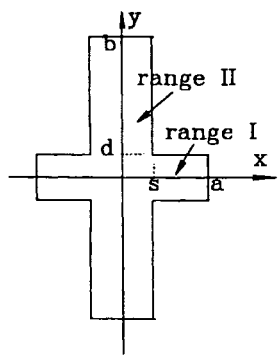

(a)

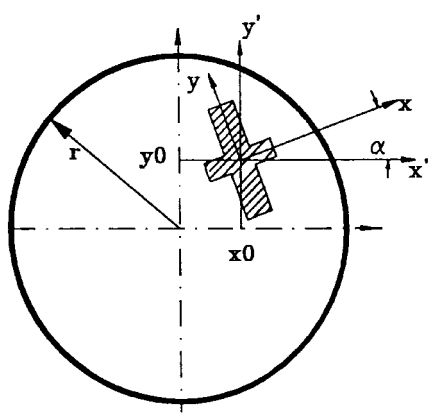

(b)

Fig. 1. (a) A symmetric crossed rectangular waveguid. (b) The general cross waveguide to large circular waveguide junction.

when (x,y) is located in range I, and

$$\vec{e}_{ht2}{}^{n} = -N_h^n \sum_r \Phi_{2m}^n \{\left(\frac{m\pi}{2b}\right) A[p_{2m}^n(\frac{x}{2a})] B[\frac{m\pi(b-y)}{2b}]\widehat{x} - \left(\frac{p_{2m}^n}{2a}\right) C[p_{2m}^n(\frac{x}{2a})] \cdot D[\frac{m\pi(b-y)}{2b}]\widehat{y}\} \tag{1c}$$

$$\vec{e}_{et2}{}^{n} = N_e^n \sum_r \Phi_{2m}^n \{\left(\frac{p_{2m}^n}{2a}\right) A[p_{2m}^n(\frac{x}{2a})] B[\frac{m\pi(b-y)}{2b}]\widehat{x} - \left(\frac{m\pi}{2b}\right) C[p_{2m}^n(\frac{x}{2a})] \cdot D[\frac{m\pi(b-y)}{2b}]\widehat{y}\} \tag{1d}$$

when (x, y) is located in range II for TE and TM modes, respectively. The functions Q, P, R, S, A, B, C, and D and boundary conditions for each mode group are listed in Table I. Since the procedure for obtaining the eigenvalues p_{1r}^n and p_{2m}^n and eigenvector coefficients Φ_{1r}^n and Φ_{2m}^n has been given in [7], it will not be discussed further here.

TABLE II
MEASURED AND CALCULATED COUPLING VALUE M FOR CROSS IRIS WITH FIXED HEIGHT $L2$ AND VARIABLE LENGTH $L1$ (IN.) FOR THE TE111 MODE

L1	Measured M	Calculated M	f_0 GHz
0.340	0.0082	0.0083	9.760
0.360	0.0100	0.0104	9.751
0.380	0.0123	0.0124	9.740
0.400	0.0151	0.0156	9.727

TABLE III
FUNCTIONS $Sign_x$ AND $Sign_y$

Quadrant k	1	2	3	4
$Sign_x(k)$	1	-1	-1	1
$Sign_y(k)$	1	1	-1	-1

B. Mode Functions in Circular Waveguide

To mode match the fields of the two waveguides at the common junction, the conventional circular cylindrical Bessel–Fourier modal functions must be converted into functions in rectangular coordinates. This is done with a finite series of exponential plane wave functions in rectangular coordinates [6]. We rewrite the (q, r) circular waveguide's modal functions [6] as follows:

$$\vec{e}_{ht2\binom{C}{S}}{}^{qr}(x', y') = N_{h,qr}{}^{(2)} \frac{h'_{qr}}{N} j^{q+1} \sum_{l=0}^{N-1} \begin{pmatrix} C_{lq} \\ S_{lq} \end{pmatrix} \cdot e^{-jh'_{qr}(C_l \cdot x_1 + S_l \cdot y_1)} \cdot (S_l \widehat{x}' - C_l \widehat{y}') e^{-jh'_{qr}(C_l \cdot x' + S_l \cdot y')} \tag{2a}$$

$$\vec{e}_{et2\binom{C}{S}}{}^{qr}(x', y') = N_{e,qr}{}^{(2)} \frac{h_{qr}}{N} j^{q+1} \sum_{l=0}^{N-1} \begin{pmatrix} C_{lq} \\ -S_{lq} \end{pmatrix} \cdot e^{-jh_{qr}(C_l \cdot x_1 + S_l \cdot y_1)} \cdot (S_l \widehat{x}' + C_l \widehat{y}') e^{-jh_{qr}(C_l \cdot x' + S_l \cdot y')} \tag{2b}$$

where $C_l q = \cos(lq\frac{2\pi}{N})$, $S_l q = \sin(lq\frac{2\pi}{N})$, $C_l = \cos(\frac{l2\pi}{N})$, and $S_l = \sin(\frac{l2\pi}{N})$. The number N of terms in the series is dictated by the argument and order of the Bessel function and has been discussed in detail in [6].

Referring to the coordinate relations shown in Fig. 1(b), we can extend (2) to incorporate a rotation angle α

$$\vec{e}_{ht2\binom{C}{S}}{}^{qr}(x, y) = N_{h,qr}{}^{(2)} \frac{h'_{qr}}{N} j^{q+1} \sum_{l=0}^{N-1} \begin{pmatrix} C_{lq} \\ S_{lq} \end{pmatrix} \cdot e^{-jh'_{qr}(C_l \cdot x_1 + S_l \cdot y_1)} \cdot (S'_l \widehat{x} - C'_l \widehat{y}) e^{-jh'_{qr}(C'_l \cdot x + S'_l \cdot y)} \tag{3a}$$

$$\vec{e}_{et2\binom{C}{S}}{}^{qr}(x, y) = N_{e,qr}{}^{(2)} \frac{h_{qr}}{N} j^{q+1} \sum_{l=0}^{N-1} \begin{pmatrix} C_{lq} \\ -S_{lq} \end{pmatrix} \cdot e^{-jh_{qr}(C_l \cdot x_1 + S_l \cdot y_1)} \cdot (S'_l \widehat{x} + C'_l \widehat{y}) e^{-jh_{qr}(C'_l \cdot x + S'_l \cdot y)} \tag{3b}$$

where $C'_l = \cos(\frac{l2\pi}{N} - \alpha)$ and $S'_l = \sin(\frac{l2\pi}{N} - \alpha)$.

Equation (3) will be the modal functions of circular waveguide to be used in the analysis.

C. Mode-Matching Equations

To obtain the mode matching equations for the junction as shown in Fig. 1(b), we enforce the fields continuity condition at the common boundary plane, that is $\vec{E}_t{}^{(1)}|_{S1} = \vec{E}_t{}^{(2)}|_{S1}$, $\vec{H}_t{}^{(1)}|_{S1} = \vec{H}_t{}^{(2)}|_{S1}$ and $\vec{E}_t{}^{(2)}|_{S2-S1} = 0$. It is assumed that S1 and S2 refer to the small and large waveguide cross sections, respectively. The above boundary conditions can be converted into a set of algebraic equations by projecting them onto some suitable functional space. A generic projection used in this paper is

$$\int_{S1} (\hat{z} \times \vec{e}_{h,kl}{}^{(1)}) \cdot \vec{H}_t{}^{(2)} ds = \int_{S1} (\hat{z} \times \vec{e}_{h,kl}{}^{(1)}) \cdot \vec{H}_t{}^{(1)} ds \tag{4a}$$

$$\int_{S1} (\hat{z} \times \vec{e}_{e,kl}{}^{(1)}) \cdot \vec{H}_t{}^{(2)} ds = \int_{S1} (\hat{z} \times \vec{e}_{e,kl}{}^{(1)}) \cdot \vec{H}_t{}^{(1)} ds \tag{4b}$$

$$\int_{S2} \vec{e}_{h,kl}{}^{(2)} \cdot \vec{E}_t{}^{(2)} ds = \int_{S1} \vec{e}_{h,kl}{}^{(2)} \cdot \vec{E}_t{}^{(1)} ds \tag{4c}$$

$$\int_{S2} \vec{e}_{e,kl}{}^{(2)} \cdot \vec{E}_t{}^{(2)} ds = \int_{S1} \vec{e}_{e,kl}{}^{(2)} \cdot \vec{E}_t{}^{(1)} ds. \tag{4d}$$

Since $\vec{E}|_t = 0$ on $\Sigma = S2 - S1$, the integrals on the right-hand side of (4c) and (4d) extend over S1. Expressing the fields in waveguide by a superposition of incident and reflected modal field series of finite length, we can rewrite (4) in a matrix form as

$$\underbrace{\begin{bmatrix} [I] & [0] & [V_{hh}^T] & [V_{he}^T] \\ [0] & [I] & [0] & [V_{ee}^T] \\ [V_{hh}] & [0] & [-I] & [0] \\ [V_{he}] & [V_{ee}] & [0] & [-I] \end{bmatrix}}_{A} \begin{bmatrix} a_h^{(1)} \\ a_e^{(1)} \\ a_h^{(2)} \\ a_e^{(2)} \end{bmatrix} = \underbrace{\begin{bmatrix} [I] & [0] & [V_{hh}^T] & [V_{he}^T] \\ [0] & [I] & [0] & [V_{ee}^T] \\ [-V_{hh}] & [0] & [I] & [0] \\ [-V_{he}] & [-V_{ee}] & [0] & [I] \end{bmatrix}}_{B} \begin{bmatrix} b_h^{(1)} \\ b_e^{(1)} \\ b_h^{(2)} \\ b_e^{(2)} \end{bmatrix} \tag{5}$$

where $V_{hh,m,n} = \sqrt{\frac{Z_{h,n}^{(1)}}{Z_{h,m}^{(2)}}} \int_{S1} \vec{e}_{hm}{}^{(2)} \cdot \vec{e}_{hn}{}^{(1)} ds$, $V_{he,m,n} = \sqrt{\frac{Z_{h,n}^{(1)}}{Z_{e,m}^{(2)}}} \int_{S1} \vec{e}_{em}{}^{(2)} \cdot \vec{e}_{hn}{}^{(1)} ds$, $V_{ee,m,n} = \sqrt{\frac{Z_{e,n}^{(1)}}{Z_{e,m}^{(2)}}} \int_{S1} \vec{e}_{em}{}^{(2)} \cdot \vec{e}_{en}{}^{(1)} ds$, vector $[a_h{}^{(i)}]$ and vector $[b_h{}^{(i)}]$ are the coefficients of the incident and reflected wave, respectively. The Z's are wave impedances of corresponding modes, and the supscript T stands for the transpose of a matrix. The general scattering matrix of the junction can be easily obtained from (5) by $[S] = [B]^{-1}[A]$.

$$\begin{aligned}\int_{S1} \vec{e}_{ht1}{}^{\bar{n}} \cdot \vec{e}_{ht2\binom{C}{S}}^{nm} ds =& N_{h\bar{n}}^{(1)} \cdot N_{h,nm}^{(2)} \frac{h_{nm}^c}{N} (j)^{n+1} \sum_l^{N-1} e^{-jh_{nm}^c[C_l x_1 + S_l y_1]} \cdot a \cdot \begin{pmatrix} C_{nl} \\ S_{nl} \end{pmatrix} \cdot \Bigg\{ d \cdot \sum_r \Phi_{1r}^{h\bar{n}} \Bigg\{ S'_l \left(\frac{r\pi}{2d}\right) \sum_{k=1}^4 A_x(k, iqq) \\ & \cdot I_1{}^c(k, a, s, h_{nm}^c \cdot C'_l, p_{1r}^{\bar{n}}) \cdot I_0{}^s(k, d, r, h_{nm}^c \cdot S'_l) + C'_l \left(\frac{p_{1r}^{\bar{n}}}{2a}\right) \sum_{k=1}^4 A_y(k, iqq) \cdot I_1{}^s(k, a, s, h_{nm}^c \cdot C'_l, p_{1r}^{\bar{n}}) \\ & \cdot I_0{}^c(k, d, r, h_{nm}^c \cdot S'_l) \Bigg\} + b \cdot \sum_q \Phi_{2q}^{h\bar{n}} \Bigg\{ S'_l \left(\frac{q\pi}{2b}\right) \sum_{k=1}^4 A_x(k, iqq) \cdot I_2{}^{\binom{s}{c}}(k, a, s, h_{nm}^c \cdot C'_l, p_{2q}^{\bar{n}}) \\ & \cdot I_0{}^s(k, b, q, h_{nm}^c \cdot S'_l) + C'_l \left(\frac{p_{2q}^{\bar{n}}}{2a}\right) \sum_{k=1}^4 A_y(k, iqq) \cdot I_2{}^{\binom{c}{s}}(k, a, s, h_{nm}^c \cdot C'_l, p_{2q}^{\bar{n}}) \cdot I_0{}^c(k, b, q, h_{nm}^c \cdot S'_l) \Bigg\} \Bigg\}\end{aligned} \tag{6a}$$

$$\begin{aligned}\int_{S1} \vec{e}_{ht1}{}^{\bar{n}} \cdot \vec{e}_{et2\binom{C}{S}}^{nm} ds =& N_{h\bar{n}}^{(1)} \cdot N_{e,nm}^{(2)} \frac{\bar{h}_{nm}^c}{N} (j)^{n+1} \sum_l^{N-1} e^{-j\bar{h}_{nm}^c[C_l x_1 + S_l y_1]} \cdot a \cdot \begin{pmatrix} C_{nl} \\ -S_{nl} \end{pmatrix} \cdot \Bigg\{ d \cdot \sum_r \Phi_{1r}^{h\bar{n}} \Bigg\{ C'_l \left(\frac{r\pi}{2d}\right) \sum_{k=1}^4 A_x(k, iqq) \\ & \cdot I_1{}^c(k, a, s, \bar{h}_{nm}^c \cdot C'_l, p_{1r}^{\bar{n}}) \cdot I_0{}^s(k, d, r, \bar{h}_{nm}^c \cdot S'_l) - S'_l \left(\frac{p_{1r}^{\bar{n}}}{2a}\right) \sum_{k=1}^4 A_y(k, iqq) \cdot I_1{}^s(k, a, s, \bar{h}_{nm}^c \cdot C'_l, p_{1r}^{\bar{n}}) \\ & \cdot I_0{}^c(k, d, r, \bar{h}_{nm}^c \cdot S'_l) \Bigg\} + b \cdot \sum_q \Phi_{2q}^{h\bar{n}} \Bigg\{ C'_l \left(\frac{q\pi}{2b}\right) \sum_{k=1}^4 A_x(k, iqq) \cdot I_2{}^{\binom{s}{c}}(k, a, s, \bar{h}_{nm}^c \cdot C'_l, p_{2q}^{\bar{n}}) \\ & \cdot I_0{}^s(k, b, q, \bar{h}_{nm}^c \cdot S'_l) - S'_l \left(\frac{p_{2q}^{\bar{n}}}{2a}\right) \sum_{k=1}^4 A_y(k, iqq) \cdot I_2{}^{\binom{c}{s}}(k, a, s, \bar{h}_{nm}^c \cdot C'_l, p_{2q}^{\bar{n}}) \cdot I_0{}^c(k, b, q, \bar{h}_{nm}^c \cdot S'_l) \Bigg\} \Bigg\}\end{aligned} \tag{6b}$$

$$\begin{aligned}\int_{S1} \vec{e}_{et1}{}^{\bar{n}} \cdot \vec{e}_{et2\binom{C}{S}}^{nm} ds =& N_{e\bar{n}}^{(1)} \cdot N_{e,nm}^{(2)} \frac{\bar{h}_{nm}^c}{N} (j)^{n+1} \sum_l^{N-1} e^{-j\bar{h}_{nm}^c[C_l x_1 + S_l y_1]} \cdot a \cdot \begin{pmatrix} C_{nl} \\ -S_{nl} \end{pmatrix} \cdot \Bigg\{ d \cdot \sum_r \Phi_{1r}^{e\bar{n}} \Bigg\{ C'_l \left(\frac{p_{1r}^{\bar{n}}}{2a}\right) \sum_{k=1}^4 A_x(k, iqq) \\ & \cdot I_1{}^c(k, a, s, \bar{h}_{nm}^c \cdot C'_l, p_{1r}^{\bar{n}}) \cdot I_0{}^s(k, d, r, \bar{h}_{nm}^c \cdot S'_l) - S'_l \left(\frac{r\pi}{2d}\right) \sum_{k=1}^4 A_y(k, iqq) \cdot I_1{}^s(k, a, s, \bar{h}_{nm}^c \cdot C'_l, p_{1r}^{\bar{n}}) \\ & \cdot I_0{}^c(k, d, r, \bar{h}_{nm}^c \cdot S'_l) \Bigg\} + b \cdot \sum_q \Phi_{2q}^{e\bar{n}} \Bigg\{ C'_l \left(\frac{p_{2q}^{\bar{n}}}{2a}\right) \sum_{k=1}^4 A_x(k, iqq) \cdot I_2{}^{\binom{s}{c}}(k, a, s, \bar{h}_{nm}^c \cdot C'_l, p_{2q}^{\bar{n}}) \\ & \cdot I_0{}^s(k, b, q, \bar{h}_{nm}^c \cdot S'_l) - S'_l \left(\frac{q\pi}{2b}\right) \sum_{k=1}^4 A_y(k, iqq) \cdot I_2{}^{\binom{c}{s}}(k, a, s, \bar{h}_{nm}^c \cdot C'_l, p_{2q}^{\bar{n}}) \cdot I_0{}^c(k, b, q, \bar{h}_{nm}^c \cdot S'_l) \Bigg\} \Bigg\}.\end{aligned} \tag{6c}$$

TABLE IV
FUNCTIONS A_x AND A_y

Quadrant k	$A_x(k,1)$	$A_x(k,2)$	$A_x(k,3)$	$A_x(k,4)$	$A_y(k,1)$	$A_y(k,2)$	$A_y(k,3)$	$A_y(k,4)$
1	1	1	1	1	1	1	1	1
2	-1	-1	1	1	1	1	-1	-1
3	1	-1	-1	1	-1	-1	1	1
4	-1	1	-1	1	1	-1	1	-1

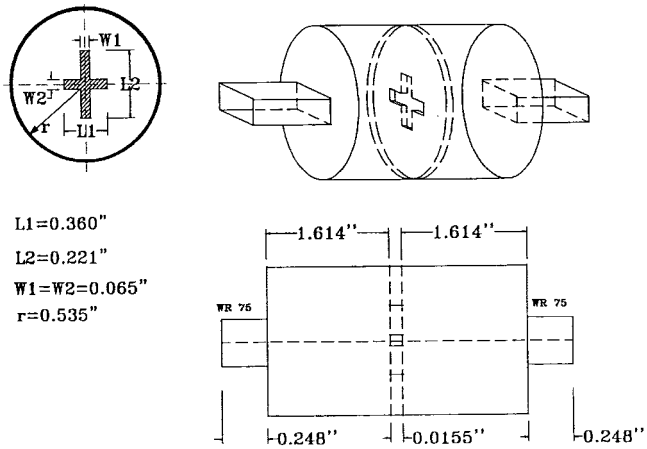

Fig. 2. A cross iris between two circular waveguide cavities.

D. Closed-Form Expressions of Matrix Elements

Referring to (1) and (3), it is straightforward to show (6a)–(6c), shown at the bottom of the previous page, where functions $I_0{}^s$, $I_0{}^c$, $I_1{}^s$, $I_1{}^c$, $I_2{}^s$, $I_2{}^c$, $A_x(k, iqq)$, and $A_y(k, iqq)$ are given in the Appendix.

III. NUMERICAL AND EXPERIMENTAL RESULTS

To verify the formulation, the structure shown in Fig. 2 is simulated, where the junction of small rectangular-to-circular waveguide is analyzed using the technique discussed in [6] and the centered cross iris is solved using the formulation discussed in this paper. It can be observed from Fig. 3 that the measured data are in very good agreement with the theoretical results.

To show the applicability of the formulation to the dual-mode waveguide filter design, the formulation developed in the previous section is used to calculated the coupling of a cross-shaped iris between two circular cavities. The coupling values of a series of centered cross irises with the same vertical slot length but different horizontal slot length $L1$ are measured to verify the formulation. The coupling values are measured by measuring the bandwidth of two circular cavities with a cross iris between them.

Table II gives the calculated and measured coupling values for the TE111 mode. The thickness of the irises is 0.016 in., the radius of circular cavity is 0.535 in., the width of the irises is 0.03 in., and the length of the vertical slot $L2$ is 0.2 in. The cavities are weakly coupled to the input/output waveguides through small apertures. Since the cavity length is fixed, the change in horizontal slot length affects the loading of the cavities and, therefore, alters the resonant frequency f_0. It has been found that only three modes are enough in the cross waveguide by using symmetrical modes in the analysis. It can be seen that the technique can be directly used in the physical dimension designing of multimode waveguide filters with very minor adjustments.

IV. CONCLUSION

A closed formulation has been developed to carry out modal analysis of small cross-to-circular waveguide junctions. The formulation is particularly useful for the analysis of a cross-shaped iris between circular waveguide cavities. Such a structure is a key element in designing multimode circular waveguide filters. The advantage of the formulation over previous work is that it can provide the coupling information for a slot in one direction in the presence of another slot in the perpendicular direction. The benefits of accuracy and efficiency are obvious from this closed-form expressions since no numerical integration is needed. The formulation has been well verified experimentally and will serve as a very useful tool for multimode circular waveguide filter design.

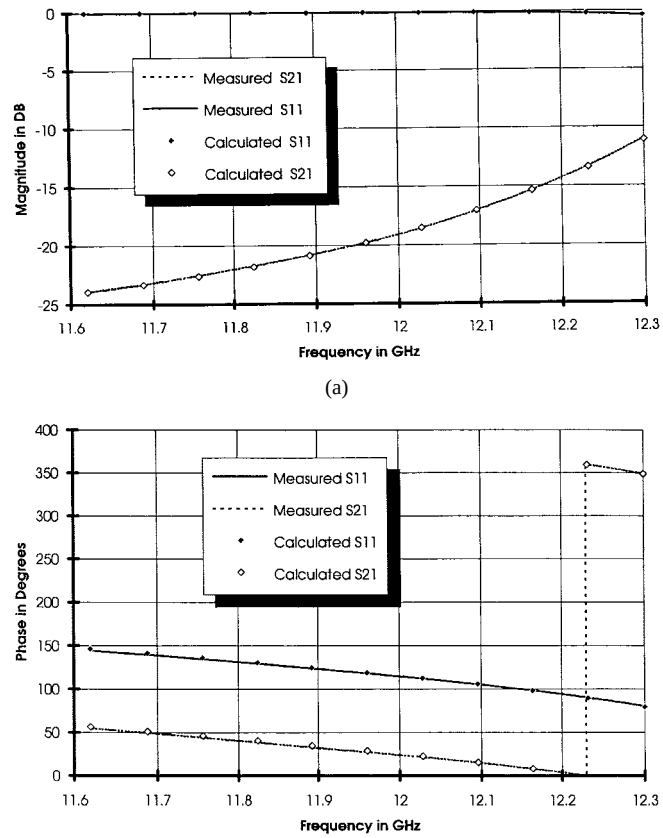

Fig. 3. (a) Measured and calculated magnitude for the structure shown in Fig. 2. (b) Measured and calculated phase for the structure shown in Fig. 2.

APPENDIX

The integrals used in (8) are defined by

$$I_0^{\substack{S\\C}}(k,d,r,h\cdot S_l) = \frac{1}{d}\int_0^d \frac{P}{S}\left[\frac{r\pi(d-y)}{2d}\right]e^{-jh\cdot S_l\cdot Sign_y(k)y}\,dy \tag{A.1}$$

$$I_1^{\substack{C\\S}}(k,a,s,h\cdot C_l,p_{1r}^{\bar{n}}) = \frac{1}{a}\int_s^a \frac{Q}{R}\left[p_{1r}^{\bar{n}}\left(\frac{x}{2a}-\frac{1}{2}\right)\right]e^{-jh\cdot C_l\cdot Sign_x(k)x}\,dx \tag{A.2}$$

and

$$I_2^{\overset{S}{C}}(k, a, s, h \cdot C_l, p_{2q}^{\bar{n}}) = \frac{1}{a}\int_0^s \overset{A}{C}[p_{2q}^{\bar{n}}(\frac{x}{2a})]e^{-jh \cdot C_l \cdot Sign_x(k)x}dx \tag{A.3}$$

all of which can be integrated analytically. As can be observed from Table III, the functions $Sign_x(k)$ and $Sign_y(k)$ (with quadrant $k = 1, 2, 3$ and 4) follow the integration direction along the x and y axes, respectively, starting from the center of the cross waveguide.

The weighting functions $A_x(k, iqq)$ and $A_y(k, iqq)$ involve the orientation information of the x- and y- components, respectively, of the modal functions in cross waveguide. The orientations of components depend on the boundary conditions of mode group (iqq) and the quadrant number (k), where the field point is located . These two functions are summarized in Table IV.

Acknowledgment

The authors would like to express their thanks to Dr. R. R. Mansour and W. C. Tang from COM DEV Ltd. for their encouragements and valuable comments on the work.

References

[1] C. Kudsia, R. Cameron, and W.-C. Tang, "Innovations in microwave filters and multiplexing networks for communications satellite systems," *IEEE Trans. Microwave Theory Tech.*, vol. 40, pp. 1133–1149, June 1992.

[2] A. E. Atia and A.E. Williams, "Narrow-bandpass waveguide filters," *IEEE Trans. Microwave Theory Tech.*, vol. MTT-20, pp. 258–265, Apr. 1972.

[3] L. Accatino and G. Bertin, "Design of coupling irises between circular cavities by modal analysis," *IEEE Trans. Microwave Theory Tech.*, vol. 42, pp. 1307–1313, July 1994.

[4] P. Couffignal, H. Baudrand, and B. Théron, "A new rigorous method for the determination of iris dimensions in dual-mode cavity filters," *IEEE Trans. Microwave Theory Tech.*, vol. 42, pp. 1314–1320, July 1994.

[5] R. Keller and F. Arndt, "Rigorous modal analysis of the asymmetric rectangular iris in circular waveguides," *IEEE Microwave Guided Wave Lett.*, vol. 3, pp. 185–187, June 1993.

[6] R. H. MacPhie and K.-L. Wu, "Scattering at the junction of a rectangular waveguide and a larger circular waveguide," *IEEE Trans. Microwave Theory Tech.*, vol. 43, pp. 2041–2045, Sept. 1995.

[7] Q. C. Tham, "Modes and cutoff frequencies of crossed rectangular waveguides," *IEEE Trans. Microwave Theory Tech.*, vol. MTT-25, pp. 585–588, July 1977.